ISSN 0001-4370, Oceanology, 2009, Vol. 49, No. 2, pp. 257–264. © Pleiades Publishing, Inc., 2009.
Original Russian Text © D.G. Levchenko, 2009, published in Okeanologiya, 2009, Vol. 49, No. 2, pp. 278–286.

MARINE GEOLOGY

Propagation of Storm Microseisms at the Ocean–Continent Boundary

D. G. Levchenko

Shirshov Institute of Oceanology, Russian Academy of Sciences, Moscow, 117218 Russia
E-mail: levch35@mail.ru

Received August 6, 2007; in final form, December 17, 2007

Abstract—Several anomalous phenomena related to the measurement of storm microseisms in northwestern Europe and on Greenland have been considered. It has been indicated that these phenomena can be explained by analyzing the microseism propagation in oceanic waveguides in the regions of abyssal plains and transformation on continental slopes of different steepness. A model of the oceanic waveguide with an inclined elastic bottom has been presented. An analysis of the family of dispersion dependences for such a model makes it possible to find an explanation for the specific features of microseism field transformation at the ocean–continent boundary into Rayleigh waves propagating on the land.

DOI: 10.1134/S0001437009020106

INTRODUCTION

Microseisms are observed in the entire frequency range of seismic signal registration and are a natural threshold limiting the sensitivity of seismographs. Extensive literature has been devoted to studying microseisms; however, many aspects of this phenomenon are still unclear. At present, it is considered established that microseisms are mainly caused by sea waves in the regions of development of large cyclones (storm microseisms). A number of researchers proposed different mechanisms by which microseisms are generated. However, a common opinion regarding the predominant location of microseism sources and propagation and transformation modes at the ocean–continent boundary is still absent. It is insufficiently known why the microseism spectral shape is stable at substantially changing microseism intensity. Several anomalous phenomena related to microseisms are also not explained. In particular, the predominant propagation of microseisms on continental slopes in some directions and absence of microseisms in other directions and the limited growth of the microseism level in coastal regions during the development of intense storms in some water areas (including the Bay of Biscay, the Greenland Sea, and the northern Atlantic in the direction of the Barents Sea [2, 4, 6, 9, 12–14, 16, 18, 19, 22, 23]) are among such phenomena.

We assume that microseisms are mainly caused in the regions of wide abyssal oceanic plans and propagate along the bottom–water surface oceanic waveguides. Such a concept makes it possible to explain many phenomena related to microseisms: propagation over large distances with an insignificant loss, the presence of stable maximums and minimums in the microseism spectra, and the wave composition of microseisms during their registration on the land and ocean floor. In the scope of this concept, the present paper considers the specific features of microseism transformation on continental slopes into surface waves propagating on the land [12].

GENERATION SOURCES AND PROPAGATION WAYS OF STORM MICROSEISMS

We should note that different researchers slightly differently interpret the concept of microseisms. Natural seismic noise in the narrow frequency ranges with periods of 4–8 and 12–18 s have been historically called microseisms (microseisms of the first and second kinds). Several works in the field of hydroacoustics consider only acoustic noise in the aquatic environment. The term "seismoacoustic noise" reflecting the close interrelation between the hydroacoustic and bottom seismic noise fields was used in other works. Since LF noise generated by sea waves propagates in the water–bottom oceanic waveguide in the form of a unified seismohydroacoustic field, for short we consider here the concept "microseisms" in order to characterize the natural noise field measured on the land, seafloor, or in a water layer in the entire studied frequency range [6, 9–11, 13].

We briefly list the well-known models of storm microseism generation in the ocean environment. As is known, the pressure caused by surface sea waves rapidly damps with increasing depth and frequency according to the formula $R = 1/\mathrm{ch}(kH)$, where R is the damping coefficient, H is the depth, and k is the wave-

number determined by the formula $\omega^2 = gk\text{th}(kH)$. The damping exceeds six orders of magnitude for a depth of 4 km at the frequencies of the microseism spectrum maximum (0.15 Hz); therefore, the direct pressure of waves on the seafloor should be taken into account only at frequencies lower than 0.01 Hz [15].

Models taking into account nonlinear processes during wave formation [2, 10, 13, 18, 21, 23] were developed in order to explain noise generation at higher frequencies. The field of homogeneous surface sources was represented as an expansion in terms of uncorrelated spatial harmonics or as the sum of the fields of independent sources with certain directional patterns [10, 17]. These models made it possible to obtain the noise field energy characteristics and to relate these characteristics to one another and to the characteristics of the sources for the case of the deep ocean.

The wave models taking into account the noise field discrete structure [3, 10, 20] were developed for a shallow sea. Two methods for specifying noise sources were also used in this case. According to one of these methods, the asymptotic representation of the point source fields was considered, and the incoherent summation of the contribution of these fields was taken in the waveguide. The other trend is based on the spectral method for expanding the field of random surface sources in terms of spatial harmonics, which can be directly related to normal waveguide modes [3, 5, 10].

We assume that the noise field in the oceanic waveguide is generated by the sum of different sources. This is indirectly confirmed by the form of the microseism distribution function, which is close to a normal distribution. In the storm zone (several hundreds of kilometers), noise can be considerably intensified due to incoherent energy accumulation in the waveguide. Since sound insignificantly damps in the marine environment, LF noise comes to a receiving point from large distances (several thousands of kilometers), being repeatedly reflected from the seafloor and surface. The present work considers the field of remote sources located in the region of abyssal plains; therefore, we can assume that a plane wave approaches the coast.

SPECIFIC FEATURES OF MICROSEISM PROPAGATION AT THE OCEAN–CONTINENT BOUNDARY

The study is based on the experimentally observed specific features of microseism propagation at the ocean–continent boundary. During the International Geophysical Year and the following years (1957–1975), special vector devices were used to measure the directions toward microseism sources at certain European seismological centers (Moscow, Vyborg, Yalta, Copenhagen, etc.). Figure 1 presents the results of these measurements. The solid lines in Fig. 1 (1) mark the sectors of the predominant direction of the microseism arrival. Arrows (2) show the average directions toward the microseism sources. Dot-and-dash arrows mark the sectors in the Pacific (TO), Atlantic (AO), and Indian (IO) oceans.

Figures 1a and 1b demonstrate the weighted directions of the microseism arrival (marked by different shading) obtained at the Nord (Greenland) and Copenhagen (Denmark) seismic stations. Microseisms predominantly arrived from the north at Copenhagen and from the southwest at Nord, which was not explained at that time.

The long-term observations indicated that microseisms almost do not come into Europe from the Gulf of Biscay region, eastern Europe, and Scandinavia from the North Atlantic region (England and the Iberian Peninsula) and to the Nord seismic station from the Greenland Sea [13, 19].

Interesting results were obtained when microseisms were studied in the Barents Sea region at the Murmansk and Barentsburg seismic stations, which make it possible to determine the direction of the seismic signals' arrival. Numerous observations indicated that the sources of the microseisms are present only in the summer and exclusively in the Barents Sea area. In the winter, when the Barents Sea is covered with ice, the level of the microseisms is very low in spite of the intense cyclones and storms in the Norwegian and North seas, which are located at small distances from this region [4, 6, 7].

The generalized results of these observations are presented on a map of northwestern Europe and the northern Atlantic (Fig. 2). Solid and dashed arrows mark the directions of the predominant and limited microseism field propagation, respectively. To explain these phenomena, we consider the bottom topography on the continental slopes and in the water areas with an anomalous propagation of microseisms.

Figure 3 demonstrates the vertical sections of the continental slopes in the indicated directions. In all the directions with an insignificant propagation of the microseism fields, the depths vary from 3.5–4 to 0.5–1 km at a slope angle larger than 5°. On the contrary, microseisms propagate more intensely in the directions with gentle slopes. For example, the western and northwestern Scandinavian continental slopes are characterized by very small angles of ascent (on average, about 0.4°) and, correspondingly, by the most intense penetration of microseisms onto the European continent. The continental slope is steep and gentle in the northern and southern Greenland regions, respectively. Therefore, microseisms come to the Nord station mostly from the south. In the Bay of Biscay region, the continental slopes are very steep, and microseisms are almost absent on the continent even during the strongest

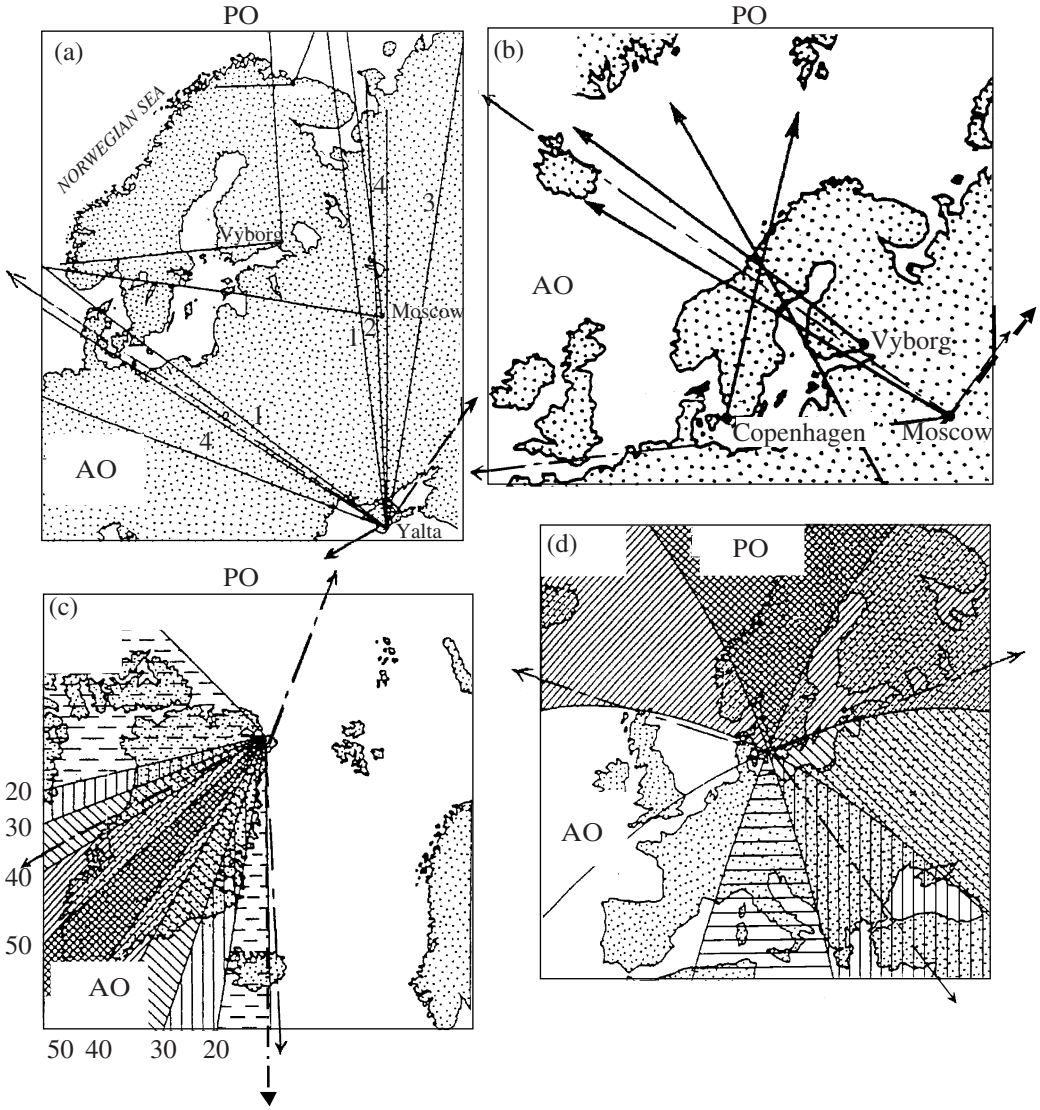

Fig. 1. Results of measuring the directions toward the sources of storm microseisms according to ((a) and (b)) Monakhov [13] and ((c) and (d)) Jensen [19]. The dot-and-dash arrows mark the sectors in the Pacific (PO) and Atlantic (AO) oceans.

cyclones. The shallow-water Barents Sea is separated from the Norwegian Sea by a threshold with a depth difference of about 2.5 km and a steepness of up to 4°. Therefore, microseisms generated by cyclones of the North and Norwegian seas do not penetrate into the Barents Sea. The steep western continental slopes of England and Ireland hinder the penetration of microseisms onto the European continent from the North Atlantic regions.

Comparing Figs. 3a and 3b, we can approximately find the critical steepness of the continental slope responsible for microseisms propagation onto the continent. Figure 4 presents the generalized inclinations of the continental slopes in the considered regions. Region I includes the slopes of increased steepness, which hinder propagation of the microseism fields. Region II includes gentle slopes where seismoacoustic fields are transformed, leave the oceanic waveguide, and further propagate along the land surface. The critical steepness of the continental slope (on average, about 3°) is apparently observed between these regions.

MODEL OF THE OCEANIC WAVEGUIDE WITH AN INCLINED ELASTIC BOTTOM

To explain the described phenomena, we consider the model of a flat oceanic waveguide with an elastic firm bottom. In such a waveguide, a normal seismoacoustic wave can be represented as a superposition of two plane waves with identical angles of incidence changing into each other when reflecting at the upper and lower boundaries. For a displacement wave, the

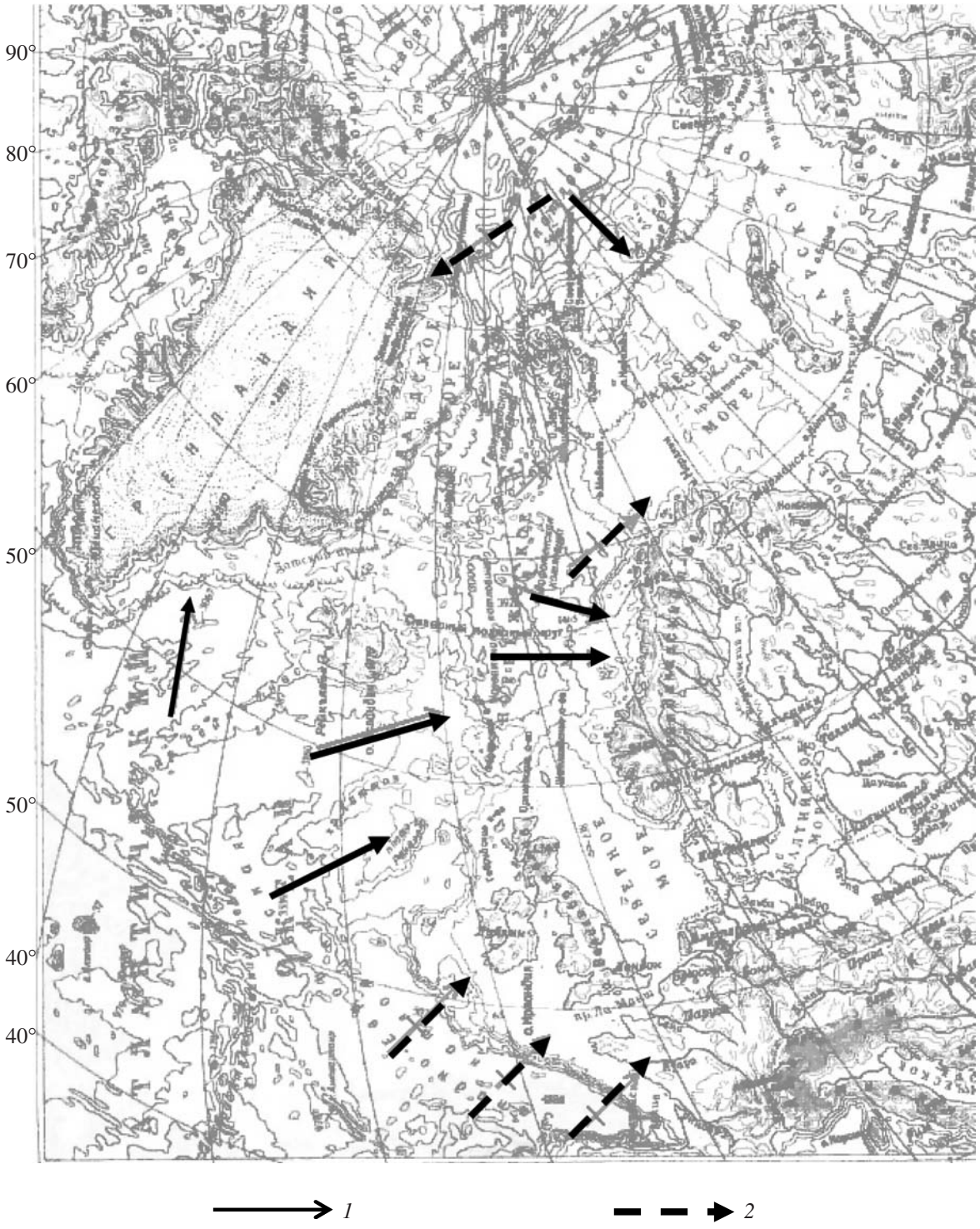

Fig. 2. Directions of the microseism field propagation in the North Atlantic regions. (*1*) predominant; (*2*) limited.

reflection coefficient (V_0) of the water–air boundary is +1 because of the large difference in the densities of the media. In the general case, the coefficient of reflection from the water–bottom boundary (V_1) has a complex character, depends on the angle of incidence, and substantially affects the conditions of the wave propagation in the waveguide [8, 22]. The following main parameters of the considered waveguide were accepted based on the generalized velocity model for the Atlantic Ocean floor [23]: the depth is H = 4000 m; the water

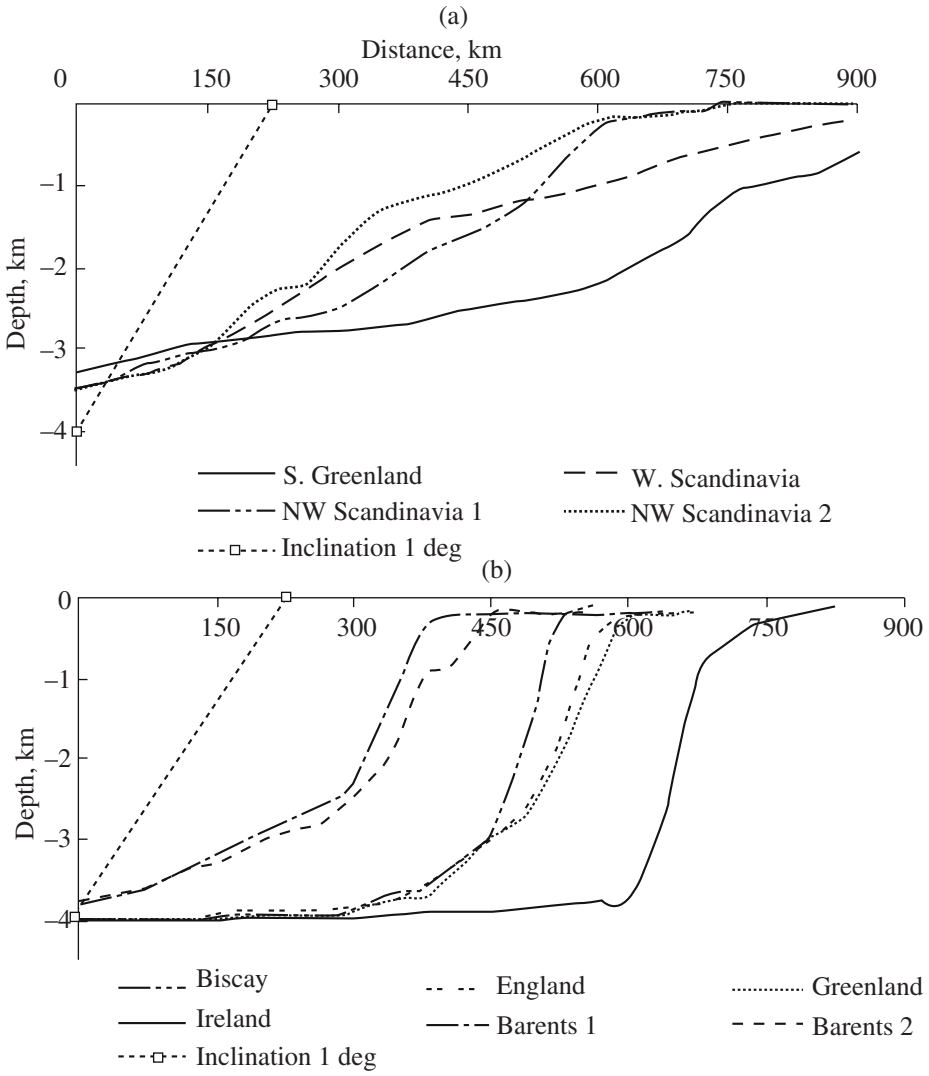

Fig. 3. Sections of the continental slopes with (a) intense and (b) limited propagation of microseisms onto the continent.

and bottom massif densities are $\rho = 1000$ km m^{-3} and $\rho_1 = 2500$ km m^{-3}, respectively; the wave velocity in water is $c = 1500$ m/s; and the longitudinal (c_l) and transverse (c_t) wave velocities in the bottom massif are 6500 and 3700 m/s, respectively.

The $c < c_t < c_l$ relationship is true in our case; therefore, we can distinguish four characteristic regions of V_1 variations:

(1) The region $0 < \theta < \theta_{krl}$, where θ_{krl} is the critical angle of incidence when the angle of refraction is $\pi/2$ for a longitudinal wave. In this region V_1 acquires real values and is substantially smaller than unity; therefore, waves do not change in the waveguide in this region of θ variations.

(2) At $\theta = \theta_{krl}$, the reflection coefficient is real and equal to unity. A longitudinal wave in the bottom massif changes into an inhomogeneous wave and propagates along the boundary as a plane surface wave. A transverse wave does not penetrate into the lower half-space. In this case, waves can propagate over large distances in a waveguide. However, the dependence of V_1 on θ is very critical (see the figure), and the region of possible deviations of θ from θ_{krl} is small.

(3) The region $\theta_{krl} < \theta < \theta_{krt}$, where θ_{krt} is the critical angle of incidence at which the angle of transverse wave refraction in the bottom massif is equal to $\pi/2$. The reflection coefficient has a complex character, and its magnitude is substantially smaller than unity due to the propagation of transverse waves in the bottom massif. In this case, waves do not propagate over large distances in a waveguide.

(4) At $\theta \geq \theta_{krt}$, the reflection coefficient has a complex character, but its magnitude is equal to unity. Longitudinal and transverse waves in a bottom massif are inhomogeneous and plane and propagate along the

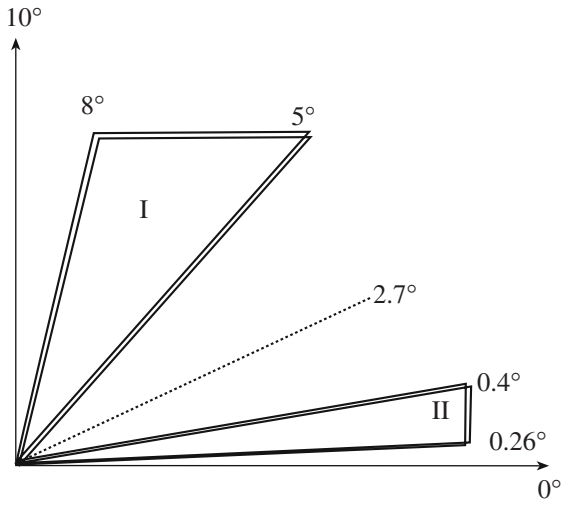

Fig. 4. Diagram of the steepness of the continental slopes with (I) limited and (II) intense propagation of microseisms.

boundary. Long-range propagation of waves in a waveguide is typical of this case.

A number of microseism propagation features can be explained by considering the dispersion relationships of the phase velocity for this oceanic waveguide model [22]. The dispersion equation for such a waveguide can be written in the following form:

$$\tan\pi\left[\frac{2H}{\lambda}(1-c^2/v^2)^{1/2}-l\right] = \left(\frac{\rho_1}{\rho}\right)(c_t^4/v^4)(v^2/c^2-1)^{1/2}(1-v^2/c_l^2)^{-1/2}[A_R], \quad (1)$$

where λ is the wavelength in water, and A_R is the characteristic expression for the Rayleigh wave; the remaining denotations are presented above.

$$A_R = 4(1-v^2/c^2)^{1/2}(1-v^2/c_t^2)^{1/2}-(2-v^2/c_t^2)^2. \quad (2)$$

The family of the dispersion dependences $v = v(H/\lambda, l)$ for the medium parameters indicated above are presented in Fig. 5. The zero mode represents part of the energy that propagates in a bottom massif in the form of a surface wave with a continuous spectrum. At $(H/\lambda) \longrightarrow 0$, the dispersion equation for this waveguide is transformed into the Rayleigh wave equation ($A_R = 0$), and ν tends to the velocity of this wave (c_R). Modes of higher orders ($l \geq 1$) propagate mostly in the water layer, form a discrete spectrum, and have critical frequencies limiting the mode frequency from below. At the critical frequencies, the phase velocity of each mode is maximal and is equal to the velocity of the shear modes in the bottom massif ($c_{1S} = c_t$).

We consider the specific features of the dispersion curves depending on the angle of incidence and frequency. According to the formulas $\sin\theta = c/v_{ph}$ and $f = c/\lambda$, for each (nonzero) mode we obtain the following situations:

(i) The flattened region, where v_{ph} varies from the maximum (c_t = 3.7 km/s) to approximately 3.3 km/s and θ changes from $\theta_{krt} = 24°$ to 27°. In this region the magnitude of the coefficient of reflection from the bottom is equal to unity, and the phase shift at the boundary is close to zero. In this case, the frequency changes from $f_{cr}(l) \approx 0.1(2l-1)$ to $f_{cr}(l+1)$Hz, where l is the mode number.

(ii) To the right of the flattened region, the v_{ph} velocity rapidly decreases and asymptotically tends to c = 1.5 km/s; θ, to $\pi/2$; and the frequency, to infinity.

(iii) For the nonzero mode, the flattened region corresponds to the propagation of the Rayleigh wave in a bottom massif in the absence of real fields in a water layer due to its small relative thickness. For the accepted parameters, this region corresponds to the frequency range from 0 to $f_{cr}(1) \approx 0.1$ Hz.

We now consider the model of microseism propagation in the regions of continental slopes (Fig. 6). We represent the continental slope in the form of a wedge with a base height of H = 4 km. Let us assume than the depth changes rather gradually; i.e., $H \ll \lambda$ at a distance equal to the wavelength λ. In this case, we can use the method of successive sections, i.e., to replace a smooth wedge with a stepped one. The real average inclinations (α) of continental slopes vary from several fractions of a degree to approximately 10° at a characteristic length (L) of several hundred kilometers. When the field propagates toward the coast, the waveguide depth decreases, and the angles of the wave incidence diminish according to the formula $\theta_n = \theta_o - 2n\alpha$, where θ_o and θ_n are the initial and final angles of incidence, and n is the number of reflections at the lower boundary. Different processes can predominate depending on the slope steepness.

(iv) At low inclinations ($\alpha < 1°$), the field propagates within angles of incidence $\theta \geq \theta_{krt}$ at $|V_1| = 1$. Adiabatic (without loss of energy) wave transformation is caused by a decrease in depth: at a decrease in H/λ, the modes of higher orders are transformed into the modes of lower orders (to the zero mode inclusive), and the field subsequently propagates on the land as a surface Rayleigh wave (see Fig. 5).

(v) At average inclinations of $1° < \alpha < 3°$, the angles of incidence $\theta < \theta_{krt}$, and the energy partly escapes into the bottom massif in the form of a shear wave and dissipates.

(vi) At steep slopes ($\alpha > 3°$), the sign of the angle of incidence can change even at a small number of reflections; i.e., part of the energy will be reflected toward the ocean.

We should note that this division of inclinations (α) was approximately performed and is true only for the

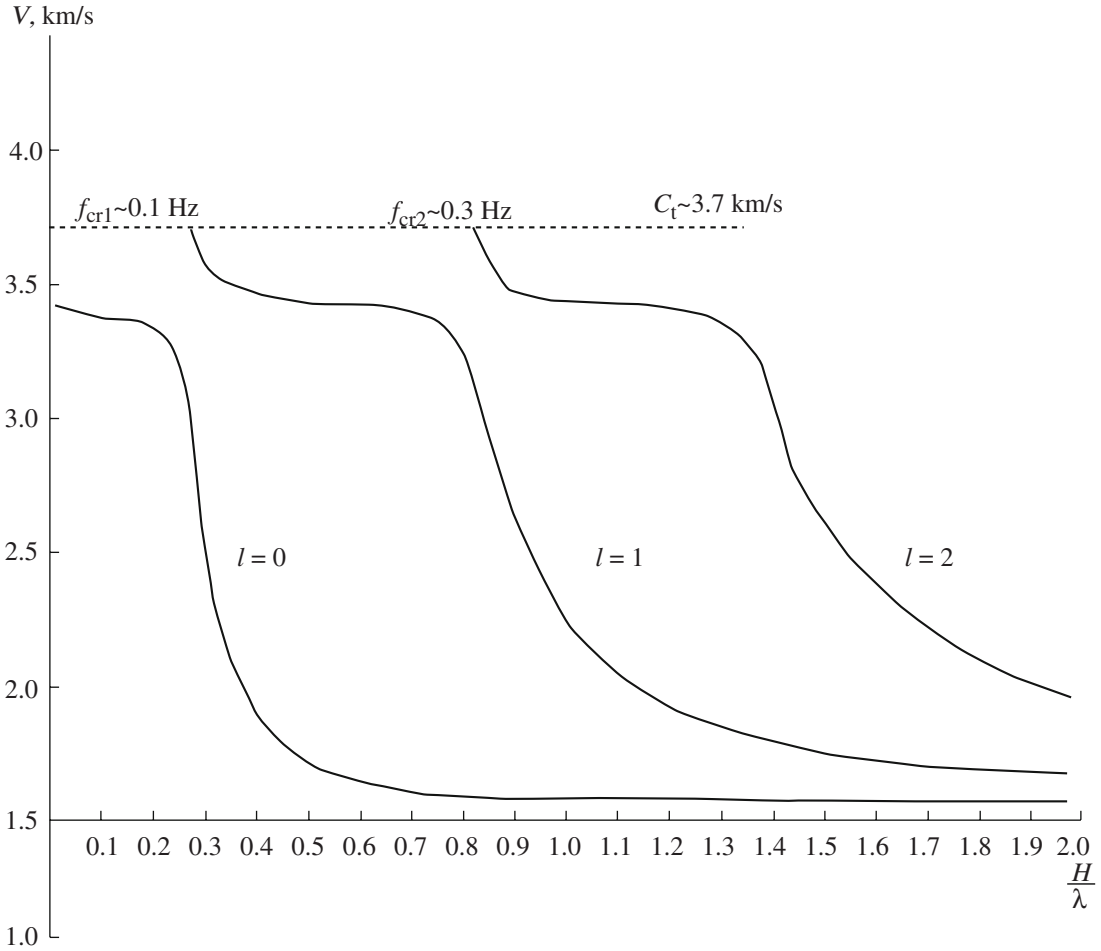

Fig. 5. Dispersion curves for an oceanic waveguide with a firm elastic bottom.

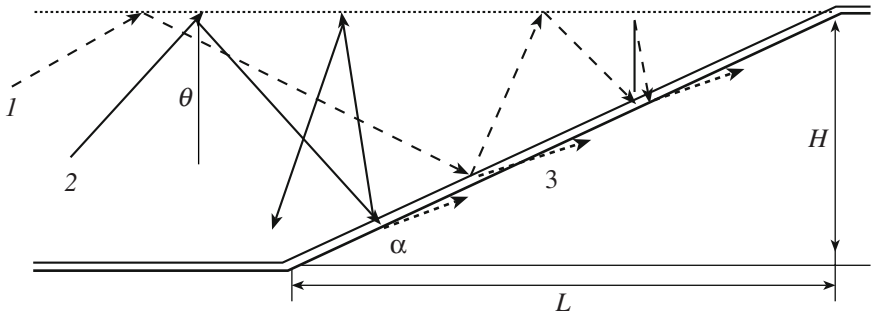

Fig. 6. The ray model of microseism propagation along a continental slope. H is the water area depth, α is the inclination, θ is the angle of the wave front incidence, (*1*) and (*2*) are the rays with different angles of incidence, (*3*) is the direction of the bottom surface wave propagation, and L is the length of the continental slope.

parameters of the presented model. However, the examples considered at the beginning of the paper indicate that this division is close to the real situations. Figure 3 presents the examples of the sections for several continental slopes in the regions with limited and predominant propagation of microseisms measured on the land. These examples confirm the considered model.

The same result can be obtained by considering the dispersion equation (1). When the depth H decreases to zero, the left-hand side of the equation vanishes, and the right-hand side changes into the characteristic equation of a Rayleigh wave.

It was experimentally established that surface Rayleigh and Love waves predominate in the composition

of microseisms. The causes of the appearance of Rayleigh waves were considered above. Rayleigh waves can be transformed into Love waves due to the Earth's crust inhomogeneities [1, 13]. However, this problem should be considered independently.

CONCLUSIONS

(1) We considered a number of the anomalous phenomena related to the propagation of storm microseisms at the ocean–continent boundary. We indicated that these phenomena can be explained by analyzing the microseism propagation in oceanic waveguides and transformation on continental slopes of different steepness.

(2) We considered the model of an oceanic waveguide with an inclined elastic bottom. An analysis of the family of depression dependences for such a model makes it possible to explain the specific features of the microseism field transformation at the ocean–continent boundary into Rayleigh waves propagating on the land.

REFERENCES

1. K. Aki and P. Richards, *Quantitative Seismology: Theory and Methods* (Mir, Moscow, 1983; Freeman, San Francisco, 1980).
2. L. M. Brekhovskikh and V. V. Goncharov, "Sound Emission by the Boundary Ocean Layer,", Ser. Akust., No. 1, 58–67 (1972).
3. L. M. Brekhovskikh and V. V. Goncharov, "Sound Generation by Surface Waves with Regard to Bottom Reflections," Izv. Akad. Nauk SSSR, Fiz. Atmos. Okeana **5** (6), 608–615 (1969).
4. L. P. Vinnik, "Structure of 4–6 s Microseisms," Dokl. Akad. Nauk SSSR **162** (5), 1041–1044 (1965).
5. Yu. L. Gazaryan, "On the Energy Spectrum of Noise in Planar Waveguides," Akust. Zh. **21** (3), 382–390 (1975).
6. N. A. Dolbilkina and O. A. Korchagina, "Specific Formation and Propagation of Microseisms in the Barents Sea and Sea of Okhotsk," Izv. Akad. Nauk SSSR, Ser. Geofiz., No. 6, 847–857 (1964).
7. N. A. Dolbilkina, T. A. Lazarenko, and V. I. Mamichev, "On the Source of Long-Period Microseisms," Fiz. Zemli, 51–54 (1967).
8. M. A. Isakovich, *General Acoustics* (Nauka, Moscow, 1973) [in Russian].
9. I. F. Kadykov, *Subsea LF Acoustic Noise* (Editorial, Moscow, 1999) [in Russian].
10. B. F. Kur'yanov, "LF Noise in Waveguides with Attenuation," in *Acoustic Waves in the Ocean* (Nauka, Moscow, 1987), pp. 184–198 [in Russian].
11. D. G. Levchenko, "Results of the Registration of Broadband (0.003–10 Hz) Seismic Signals on the Sea Bottom," Okeanologiya **42** (4), 620–631 (2002) [Oceanology **42** (4), 594–605 (2002)].
12. D. G. Levchenko, *Registration of Broadband Seismic Signals and Possible Precursors of Strong Earthquakes on the Sea Bottom* (Nauch. Mir, Moscow, 2005) [in Russian].
13. F. I. Monakhov, *LF Seismic Noise of the Earth* (Nauka, Moscow, 1977) [in Russian].
14. A. A. Ostrovskii, *Bottom Seismic Experiments* (Nauka, Moscow, 1998) [in Russian].
15. A. B. Rabinovich, *Long Gravity Waves in the Ocean: Trapping, Resonance, Emission* (Gidrometeoizdat, St. Petersburg, 1993) [in Russian].
16. S. L. Solov'ev, *Seismological Bottom Observations in the USSR and Abroad* (Nauka, Moscow, 1986) [in Russian].
17. B. F. Cron and C. N. Sherman, "Spatial-Correlation Function for Various Noise Models," JASA **34** (11), 1132–1136 (1962).
18. K. A. Hasselmann, "A Statistical Analysis of the Generation of Microseisms," Rev. Geophys. **1** (2), 177–210 (1963).
19. H. Jensen, *Statistical Studies on IGY Microseisms from Kobenhavn and Nord. Kobenhavn* (Elsevier, Amsterdam, 1961).
20. W. A. Kuperman and F. Ingenito, "Spatial Correlation of Surface Generated Noise in a Stratified Ocean," JASA **67** (6), 1988–1996 (1980).
21. Longuet-Higgins M.S. "A Theory of Origin of Microseisms," Phil. Trans. R. Soc. London, (1950).
22. F. Press and M. Ewing, "A Theory of Microseisms with Geologic Applications," Trans. Am. Geophys. Un. **29** (3), 163–174 (1948).
23. S. C. Webb, "The Equilibrium Oceanic Microseism Spectrum," JASA **92** (4) Part 1, 2141–2157 (1992).